Stage-specific dual function: EZH2 regulates human erythropoiesis by eliciting histone and non-histone methylation

Mengjia Li,[1*] Donghao Liu,[1*] Fumin Xue,[2*] Hengchao Zhang,[1] Qianqian Yang,[1] Lei Sun,[1] Xiaoli Qu,[1] Xiuyun Wu,[1] Huizhi Zhao,[1] Jing Liu,[3] Qiaozhen Kang,[1] Ting Wang,[1] Xiuli An[4#] and Lixiang Chen[1#]

[1]School of Life Sciences, Zhengzhou University, Zhengzhou, China; [2]Department of Gastroenterology, Children's Hospital affiliated to Zhengzhou University, Zhengzhou, China; [3]Molecular Biology Research Center and Center for Medical Genetics, School of Life Sciences, Central South University, Changsha, China and [4]Laboratory of Membrane Biology, New York Blood Center, New York, NY, USA

[*]ML, DL and FX contributed equally as first authors.
[#]XA and LC contributed equally as senior authors.

Correspondence: L. Chen
lxchen@zzu.edu.cn

X. An
xan@nybc.org

Received: September 5, 2022.
Accepted: March 28, 2023.
Early view: April 6, 2023.

https://doi.org/10.3324/haematol.2022.282016

©2023 Ferrata Storti Foundation
Published under a CC BY-NC license

Supplementary Methods

Antibodies.

Antibodies for flow cytometric analysis were used as follows: PE-conjugated CD34 (#555822, BD), FITC Mouse Anti-Human CD36 (#555454, BD), PE-Cy™7 Mouse Anti-Human CD123 (#560826, BD), APC-conjugated CD235a/GPA (#551336, BD). Antibodies of erythroid precursor cells were purchased as follows: PE-conjugated CD235a/GPA (#555570, BD), APC-conjugated α4-integrin (#130-124-229, MACS) The mouse monoclonal antibody against human Band 3 was generated in our laboratory and labeled with FITC. APC-conjugated Annexin V (#88-8103-74, eBioscience), Hoechst 33342 (#C0031, Solarbio), and 7AAD (#00-6993-50, eBioscience) were purchased as described. Antibodies used for western blotting and immunofluorescence were purchased as follows: mouse anti-human GAPDH (#60004-1-Ig, Proteintech), mouse anti-human β-Tubulin (10094-1-AP, Proteintech). Both anti-HSP70 (sc-24) and anti-HSP90 (sc-7947) antibodies were purchased from Santa Cruz Biotechnology. Rabbit anti-human RCC1 (ab152156) and anti-methylated lysine (Methyl K) (ab23366) antibodies were purchased from Abcam. EZH2 (#5246S), HSP70 (#4873S), Histone H3 (#4499), Tri-Methyl-Histone H3 (Lys27) (C36B11) Rabbit mAb (#9733S), and mAb IgG XP® Isotype Control (#3900) antibodies were purchased from Cell Signaling Technology.

Culture of $CD34^+$cells

The cell culture details have been described previously[1]. The details were as follows: The day of getting $CD34^+$ cells was recorded as day 0. The cell culture procedure was comprised of 3 phases. Composition of the base culture medium was Iscove's Modified Dulbecco's Medium, 2% human peripheral blood plasma, 3% human AB serum, 200 mg/mL human Holo-transferrin, 3 IU/mL heparin, and 10 mg/mL insulin. In the first phase (day 0 to day 6), $CD34^+$ cells at a concentration of 10^5 /mL were cultured in the presence of 10 ng/mL stem cell factor, 1 ng/mL IL-3, and 3 IU/mL erythropoietin. In the second phase (day 7 to day 11), IL-3 does not need to be added into the culture medium. In the third phase that lasted until day 21, the cell concentration was adjusted to 10^6 /mL on day 11 and to 5×10^6/mL on day 15, respectively, the medium for this phase was the base medium plus 3 IU/mL erythropoietin, and the concentration of transferrin was adjusted to 1 mg/mL.

RNA extraction and quantitative reverse transcription-PCR assays.

RNA was extracted from cell cultures using RNA extract kits (74104, Qiagen)

according to the manufacturer's instructions. Then reverse transcription was performed using HiFi-MMLV cDNA Kit (CW0744M, CWBIO). Quantitative reverse transcription-PCR was carried out on Light Cycler 480 instrument (Roche Life Science) using Master mix according to the manufacturer's[1] instructions Relative expression levels were normalized to *GAPDH*. The sequences are listed in Supplemental Table 1.

Protein extract.

Total cell lysates were prepared with RIPA buffer (89900, Thermo Fisher Scientific) in the presence of the proteinase inhibitor phenylmethanesulfonyl fluoride (PMSF) (#36978, Thermo Fisher Scientific). Cytoplasm and nuclear protein extraction were preformed using a NE-PER™ Nuclear and Cytoplasmic Extraction Reagent kit (#76833, Thermo Fisher Scientific). The protein concentration of the lysates was determined using the Micro BCA™ Protein Assay Kit (23235, Thermo Fisher Scientific).

Cytospin assay.

Cells (0.1×10^6) were suspended in 200 μL PBS and then adhered to a slide by Cytospin centrifugation. Slides were then stained with May-Grünwald (MG500, Sigma) solution for 5 minutes. Then slides were washed with 40 mM tris buffer (pH 7.2) for 90 seconds, the slides were immediately stained with Giemsa solution (GS500, Sigma) for 15 minutes. The images were finally taken using a standard light microscope (Axio Imager.A2, Carl Zeiss Microscopy GmbH, Jena, Germany).

Colony-forming assay.

Cells (2000) were collected and suspended in 1 mL StemSpan™ Serum-Free Expansion Medium (SFEM) and then seeded in methylcellulose medium supplemented with recombinant cytokines and erythropoietin (EPO) (MethoCult H4434, Stem Cell Technologies) for a BFU-E colony assay or methylcellulose medium with EPO only (MethoCult H4330, Stem cell Technologies) for a CFU-E colony assay. CFU-E colonies and BFU-E colonies were observed and counted under an inverted microscope (Primo Vert, Carl Zeiss Microscopy GmbH, Jena, Germany) on day 7 or day 14.

Immunofluorescence.

Cells (0.5×10^6) were collected and suspended in 1.5 mL of PBS buffer. After centrifugation at 400 × g at 4°C for 5 minutes, the cell pellet was collected. Then the cells were fixed with 4% paraformaldehyde at 25°C for 10 minutes and permeabilized with 0.1% Triton X-100 for 10 minutes. Cells were then incubated in 10% horse serum and 0.1% Triton X-100 in PBS for 30 minutes to minimize nonspecific antibody binding.

Cells were incubated with primary antibodies at 4°C for 12 hours, washed three times with PBS, and incubated with the appropriate second antibody at 25°C for 2 hours. After washing three times with PBS to remove nonspecific staining, the cells were collected and seeded onto a Thermo Scientific™ Nunc™ Lab-Tek™ II chamber (#155382). Images were collected on a confocal laser scanning microscope with a ×100 oil objective lens (Zeiss LSM780, Carl Zeiss Microscopy GmbH, Jena, Germany).

Cell cycle assay.

An EdU flow cytometry assay kit (Invitrogen, No. MAN0009883) was used for cell cycle detection according to the manufacturer's protocol.

Flow cytometric analysis.

Differentiation, apoptosis, cell cycle, and enucleation of erythroid cells were assessed using previously identified surface markers via BD LSRFortessa™ flow cytometry[1].

Chromatin immunoprecipitation (ChIP).

ChIP assay were performed according to the instruction manual of the SimpleChIP® Enzymatic Chromatin IP Kit (#9003, Cell Signaling Technology). Cells (20×10^6) were collected and cross-linked with 1% formaldehyde for 10 minutes, and then quenched with 125 mM glycine by gentle shaking for 5 minutes at 25°C. Cells were quickly rinsed twice with cold PBS and collected in PBS supplemented with protease inhibitors. The cells were then centrifuged and lysed in ice-cold lysis buffer (1% SDS, 5 mM EDTA, 50 mM Tris-HCl, pH 8.1) supplemented with protease inhibitor for 10 minutes. Cell lysates were sonicated using a Bioruptor Sonicator (01D868, Scientz) to split the DNA into fragments that were approximately 300 base pairs (bp) (approximately 500 bp for ChIP quantitative PCR (qPCR)) in length. Soluble chromatin was diluted in dilution buffer (1% Triton X-100, 2 mM EDTA, 150 mM NaCl, 20 mM Tris-HCl, pH 8.1), and 2–10 μg of antibody pre-conjugated to ChIP-Grade Protein G Magnetic Beads was added and incubated for 12 hours with gentle shaking at 4°C. The antibody used specifically for H3K27me3 (#9733, Cell signaling technology). DNA binding buffer (#10008, Cell Signaling Technology) and DNA purification columns and collection tubes (#10010, Cell Signaling Technology) were used to obtain the purified ChIP DNA.

ChIP-seq data processing.

Libraries were constructed using Hiseq × Ten Reagent kit v2.5 (#FC-501-2501, Illumina) and then sequenced on an Illumina X-ten (E00487, Illumina). Reads from the ChIP-seq data were compared to the reference genome hg19 using Bowtie2 version 2.3.5.1 software[2] (https://sourceforge.net/projects/bowtie-bio/files/bowtie2/2.3.5.1/),

and only unique and non-duplicate mapped reads were used for downstream analysis. Samtools version 1.6 software[3] (https://github.com/samtools/samtools/releases/) was used to measure the coverage and depth of reads. To check the reproducibility of ChIP-seq experiments, deeptools version 2.5.7 (https://deeptools.readthedocs.io/en/develop/content/installation.html) was used to generate correlation plots for all samples. Signal trace files in BigWig format were generated using deeptools software[4] and normalized to 1 million reads for visualization. Deeptools software was also used to normalize signal intensity, map gene body, and flanking region heatmap. Peaks and annotation were performed using ChIPseeker version 1.2.0[5] (https://www.bioconductor.org/packages/3.9/bioc/html/ChIPseeker.html). Functional analysis of genes associated with differential peaks was performed using internal scripts, such as Gene Ontology (GO, http://geneontology.org/) and Kyoto Encyclopedia of Genes and Genomes (KEGG, (http://www.kegg.jp/) analysis. Motif analysis was performed by Hypergeometric Optimization of Motif Enrichment (HOMER) tool Homer version 4.11 (http://homer.ucsd.edu/homer/).

RNA-seq and bioinformatics analysis.

Cells (2×10^6) were collected and washed twice with PBS. RNA was extracted and used as the input. The cDNA library was prepared using NovaSeq 5000/6000 S4 Reagent Kit (#A00358, Illumina) and sequenced on an Illumina X-ten (E00487, Illumina). The original data were filtered and compared with the reference genome hg19. HTSeq[6] was used to read the counts for each gene in each sample, and then FPKM (Fragments Per Kilobase Million Mapped Reads) was calculated to evaluate the expression level. DEseq2 version 1.6.3 software[7] (https://bioconductor.org/packages/3.0/bioc/html/DESeq2.html) and edgeR version 3.26.8 software[8] (https://bioconductor.org/packages/3.9/bioc/html/edgeR.html) were used to identify differentially expressed genes from the data. The GO and KEGG databases were used for the functional enrichment analysis. Gene Set Enrichment Analysis (GSEA) was performed using GSEA version 4.1.0 software[9] (http://www.gsea-msigdb.org/gsea/downloads.jsp).

References

1. Hu J, Liu J, Xue F, et al. Isolation and functional characterization of human erythroblasts at distinct stages: implications for understanding of normal and

disordered erythropoiesis in vivo. Blood. 2013;121(16):3246-3253.

2. Langmead B, Salzberg S. Fast gapped-read alignment with Bowtie 2. Nat Methods. 2012;9(4):357-359.
3. Li H, Handsaker B, Wysoker A, et al. The Sequence Alignment/Map format and SAMtools. Bioinformatics. 2009;25(16):2078-2079.
4. Ramírez F, Dündar F, Diehl S, Grüning BA, Manke T. deepTools: a flexible platform for exploring deep-sequencing data. Nucleic Acids Res. 2014;42(Web Server issue):W187-W191.
5. Yu G, Wang LG, He Q. ChIPseeker: an R/Bioconductor package for ChIP peak annotation, comparison and visualization. Bioinformatics. 2015;31(14):2382-2383.
6. Anders S, Pyl PT, Huber W. HTSeq--a Python framework to work with high-throughput sequencing data. Bioinformatics. 2015;31(2):166-169.
7. Love MI, Huber W, Anders S. Moderated estimation of fold change and dispersion for RNA-seq data with DESeq2. Genome Biol. 2014;15(12):550.
8. Robinson MD, McCarthy DJ, Smyth G. edgeR: a Bioconductor package for differential expression analysis of digital gene expression data. Bioinformatics. 2010;26(1):139-140.
9. Subramanian A, Tamayo P, Mootha VK, et al. Gene set enrichment analysis: a knowledge-based approach for interpreting genome-wide expression profiles. Proc Natl Acad Sci U S A. 2005;102(43):15545-15550.

Supplementary Figures

Supplemental Figure 1. Cell composition of each cell category. (A) Cell composition of each cell category determined using flow cytometry. scale bar, 5 μm. **(B)** Representative cytospin images showing the cell morphology of the cultured erythroid cells on days 7, 9, 11, 13, and 15. Statistical analysis is from 3 independent experiments, and the bar plot represents mean ± SD of triplicate samples. Not significant (ns), * $p < 0.05$, ** $p < 0.01$, *** $p < 0.001$.

Supplemental Figure 2. The expression level of EZH2 during erythropoiesis. RNA-seq data showing the expression level of EZH2 during each erythroblast stage, which were cultured from normal human (**A)** cord blood cells and **(B)** peripheral blood cells. Statistical analysis is from 3 independent experiments, and the bar plot represents mean ± SD of triplicate samples. Not significant (ns), * $p < 0.05$, ** $p < 0.01$, *** $p < 0.001$.

Supplemental Figure 3. The knockdown efficiency of EZH2. (A) qRT-PCR results showing EZH2 expression in erythroblasts infected with lentivirus containing Scramble-shRNA and EZH2-shRNA on day 7. The results were normalized to GAPDH mRNA. **(B)** Representative western blot images showing the knockdown efficiency of Scramble-shRNA and EZH2-shRNA on day 7. **(C)** Quantitative analysis of the knockdown efficiency of EZH2 from three independent experiments. The results were normalized to GAPDH protein. Statistical analysis is from 3 independent experiments, and the bar plot represents mean ± SD of triplicate samples. Not significant (ns), * $p < 0.05$, ** $p < 0.01$, *** $p < 0.001$.

Supplemental Figure 4. Knockdown of EZH2 have no effect on cell apoptosis. (A) Representative flow cytometry profiles of apoptosis in cells transfected with Scramble-shRNA, EZH2-shRNA and treated with or without EPZ6438 (0.5 μM, 5 μM) and stained with 7-AAD and Annexin V on day 7 of culture**. (B)** Quantitative analysis of apoptotic cells from three independent experiments, and the bar plot represents mean ± SD of triplicate samples. Not significant (ns), * $p < 0.05$, ** $p < 0.01$, *** $p < 0.001$.

Supplemental Figure 5. Correlation analysis of ChIP-seq and RNA-seq. (A) Principal component analysis (PCA) of ChIP-seq data. **(B)** Pearsons correlation analysis of ChIP-seq. **(C)** Principal component analysis (PCA) of RNA-seq data. **(D)** Pearsons correlation analysis of RNA -seq.

Supplemental Figure 6. Differential analysis of ChIP-seq. (A) The bar plot showing the distribution of different peaks relative to gene features. **(B)** The volcano map

showing upregulation (red color) and downregulation (blue color) of gene expression. **(C)** The heat map showing difference of genes comparing Scramble-shRNA and EZH2-shRNA.

Supplemental Figure 7. GO pathway enrichment analysis of RNA-seq. (A) Top 15 upregulated pathways in EZH2-shRNA group. **(B)** Top 15 downregulated pathways in EZH2-shRNA group. The color represents log transformed adjusted p-value; the width indicates the number of differentially expressed genes in the category.

Supplemental Figure 8. Integrated analysis of ChIP-seq and RNA-seq. (A) Heat meap of ChIP-seq and RNA-seq showed decreased H3K27me3 signal around transcription start site (TSS) and upregulated CDK gene expression in EZH2-shRNA group. **(B)** The normalized count value of (a) CDKN1A and (b) CDKN1C in Scramble-shRNA and EZH2-shRNA from RNA-seq as indicated. **(C)** Quantitative analysis of the relative mRNA expression level of (a) CDKN1A and (b) CDKN1C from three independent experiments. Statistical analysis is from 3 independent experiments, and the bar plot represents mean ± SD of triplicate samples. Not significant (ns), *$p < 0.05$, **$p < 0.01$, ***$p < 0.001$.

Supplemental Figure 9. EZH2-knockdown did not impair cell growth or apoptosis during terminal erythropoiesis. (A) Growth curves of cells, including Scramble-shRNA, EZH2-shRNA, DMSO control, EPZ6438-0.5 μM, and EPZ6438-5 μM. **(B)** Representative flow cytometry profiles of apoptosis by staining with 7-AAD and Annexin V on days 13 and 15 of culture cells transfected with Scramble-shRNA and EZH2-shRNA and treated with or without EPZ6438 (0.5 μM, 5 μM)**. (C)** Representative flow cytometry profiles of cell cycle as assessed by EdU and 7-AAD staining of day 15 erythroid cells. **(D)** Quantitative analysis of apoptotic cells from three independent experiments. **(E)** Quantitative analysis of the cell cycle from three independent experiments. Statistical analysis is from 3 independent experiments, and the bar plot represents mean ± SD of triplicate samples. Not significant (ns), * $p < 0.05$, ** $p < 0.01$, *** $p < 0.001$.

Supplemental Figure 10. EZH2-knockdown has no effect on terminal erythroid differentiation. (A) Flow cytometry analysis showing the percentage of GPA-positive cells on days 9, 11, 13, and 15. **(B)** Quantitative analysis of GPA-positive cells from three independent experiments. **(C)** Representative images of Scramble-shRNA, EZH2-shRNA, DMSO control, EPZ6438-0.5 μM, and EPZ6438-5 μM on days 9, 11, 13, and 15, abnormal nuclear cells as shown by red arrows; scale bar, 5 μm. **(D)** Flow

cytometry analysis showing the expression of α4 integrin and band 3 of erythroid cells cultured for days 9, 11, 13, and 15. **(E)** Quantitative analysis of the percentage of cells in each stage from three independent experiments; (1) day 9, (2) day 11, (3) day 13, and (4) day 15; Statistical analysis is from 3 independent experiments, and the bar plot represents mean ± SD of triplicate samples. Not significant (ns), * $p < 0.05$, ** $p < 0.01$, *** $p < 0.001$.

Supplemental Figure 11. Mass spectrometry analysis of HSP70 peptide with HSP70 incubation. Mass spectrometry analysis of HSP70 peptide with HSP70 incubation at D15 in culture cells with control and EZH2-knockdown group. The data was analyzed using the software Proteome Discoverer 1.4, and the peptides and sites at which HSP70 was methylated are shown in the upper right corner, and the sites are **(A)** Lys10, **(B)** Lys33, **(C)** Lys7, Lys9. **(D)** The table shows the sequence and site of HSP70 methylation.

Supplemental Figure 12. AURKB had no effect on cell apoptosis and differentiation during the terminal erythropoiesis. (A) Representative flow cytometry profiles of apoptosis by staining with 7AAD and Annexin V at D13 and D15 in culture cells treated with or without AZD2811 (2 nM, 10 nM). **(B)** Quantitative analysis of apoptotic cells from three independent experiments. **(C)** Flow cytometric analysis showing the expression of α4 integrin and band 3 of erythroid cells cultured for days 13 and 15. **(D)** Quantitative analysis of the percentage of cells in each stage from three independent experiments. Statistical analysis is from 3 independent experiments, and the bar plot represents mean ± SD of triplicate samples. Not significant (ns), * $p < 0.05$, ** $p < 0.01$, *** $p < 0.001$.

Supplemental Figure 13. Knockdown EZH2 have no effect on the expression of GATA1. (A) RNA-seq data showing the expression level of GATA1 on day 15 of Scramble-shRNA and EZH2-shRNA. **(B)** Representative western blots showing the levels of GATA1 on day 15 of Scramble-shRNA and EZH2-shRNA. **(C)** Quantitative analysis of EZH2 protein level from three independent experiments. Statistical analysis is from 3 independent experiments, and the bar plot represents mean ± SD of triplicate samples. Not significant (ns), * $p < 0.05$, ** $p < 0.01$, *** $p < 0.001$.

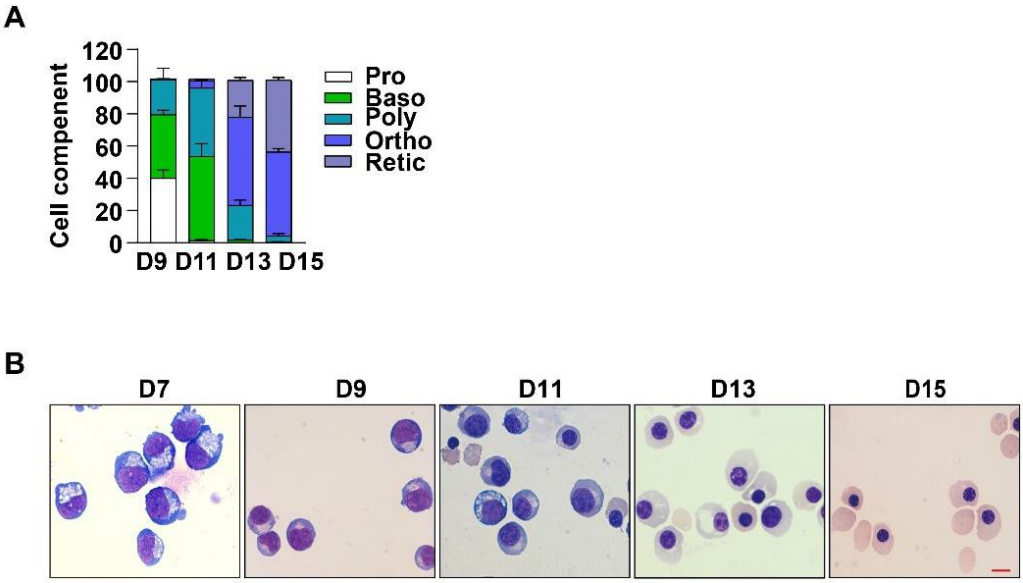

Supplemental Figure 1. Cell composition of each cell category

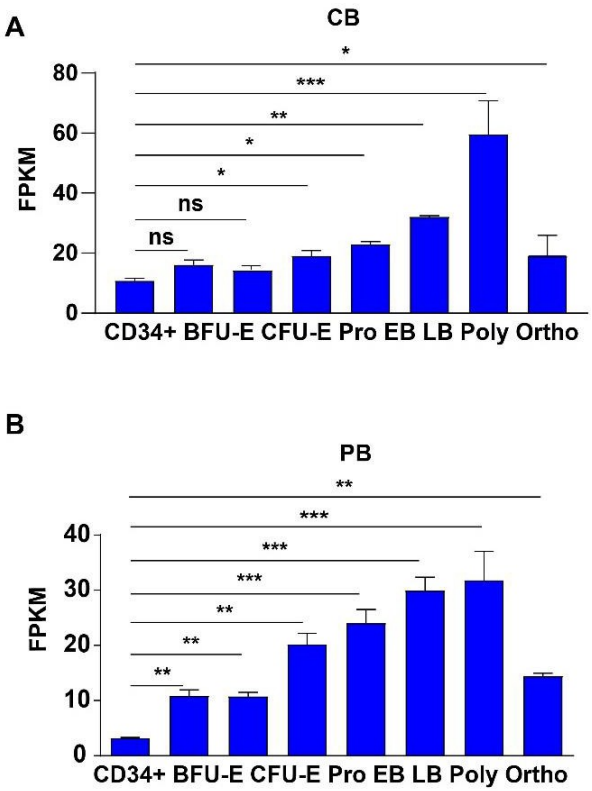

Supplemental Figure 2. The expression level of EZH2 during erythropoiesis

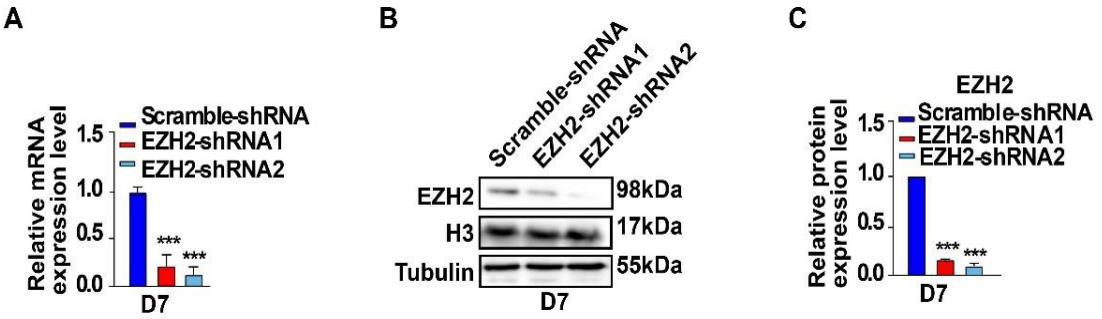

Supplemental Figure 3. The knockdown efficiency of EZH2.

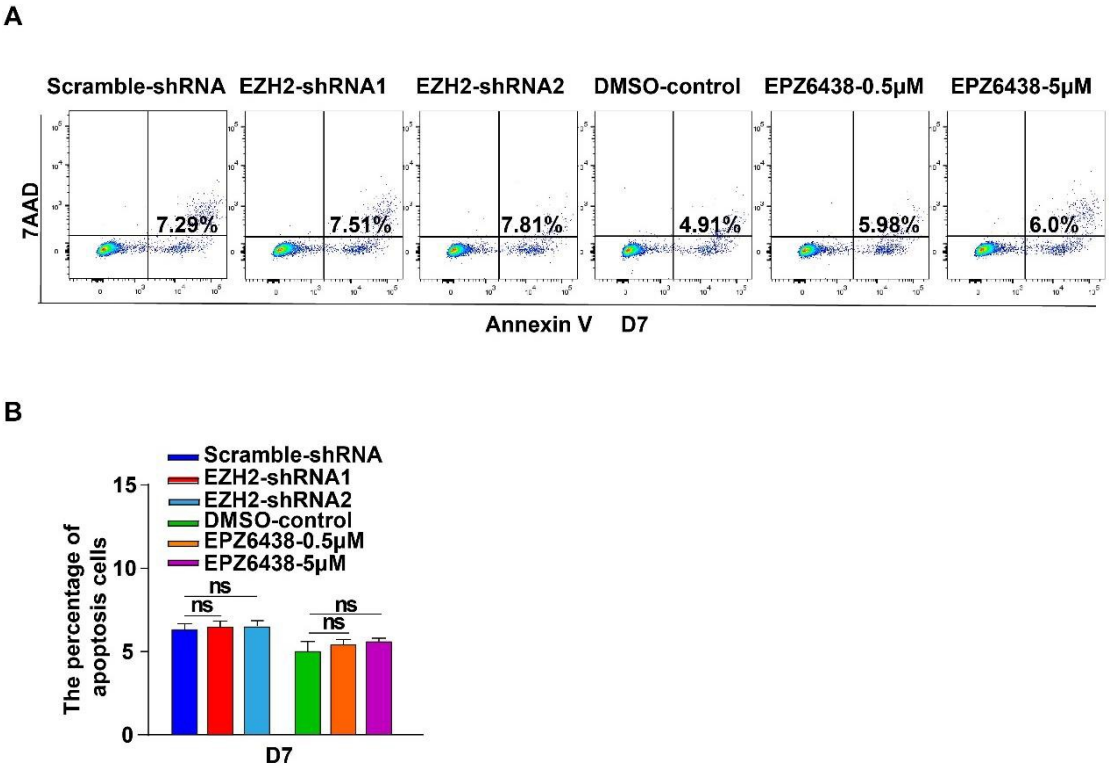

Supplemental Figure 4. Knockdown of EZH2 have no effect on cell apoptosis

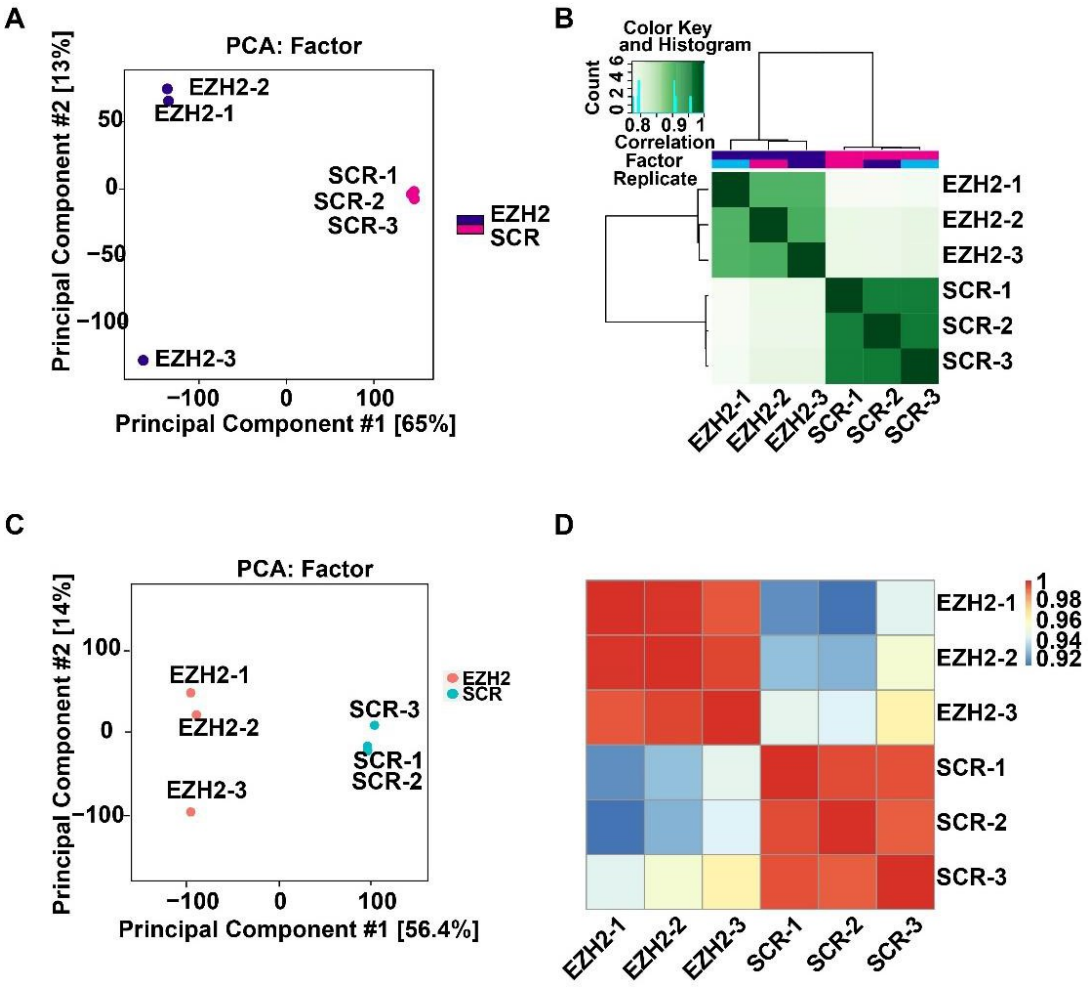

Supplemental Figure 5. Correlation analysis of ChIP-seq and RNA-seq

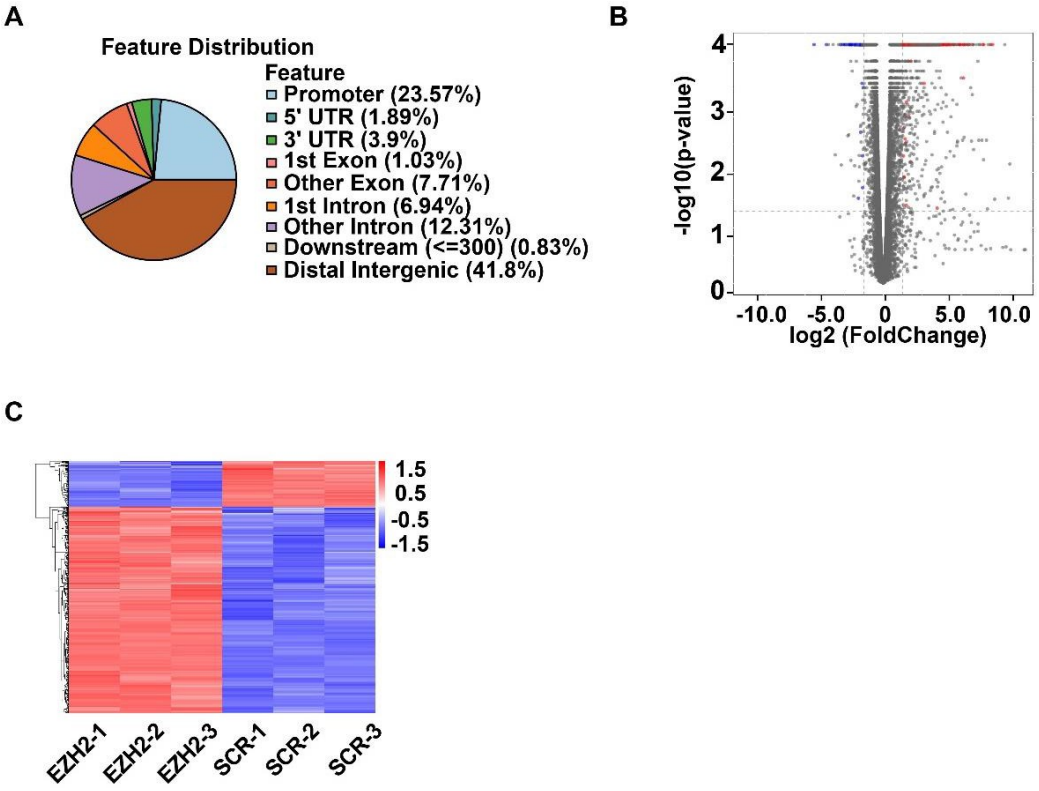

Supplemental Figure 6. Differential analysis of ChIP-seq

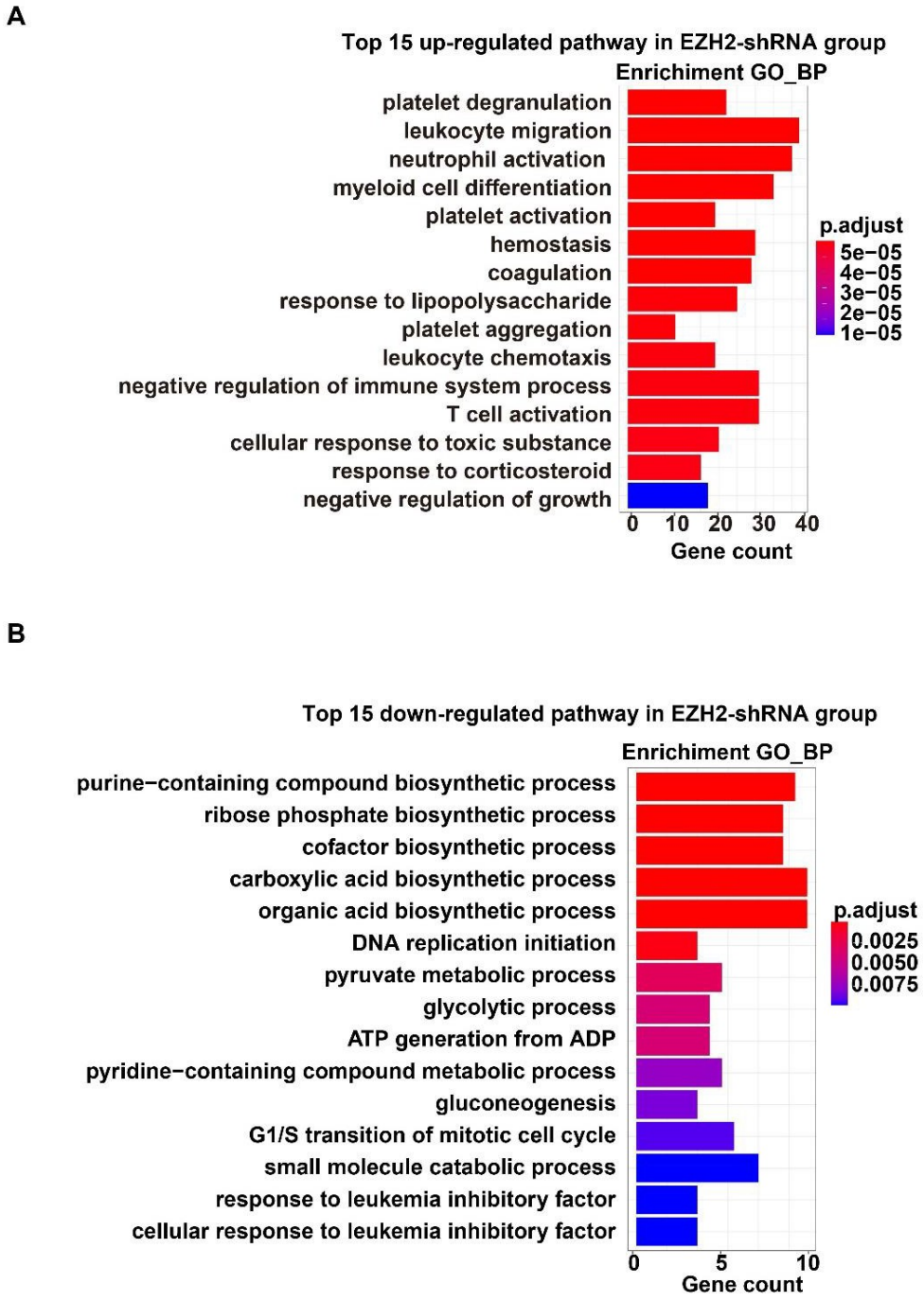

Supplemental Figure 7. GO pathway enrichment analysis of RNA-seq

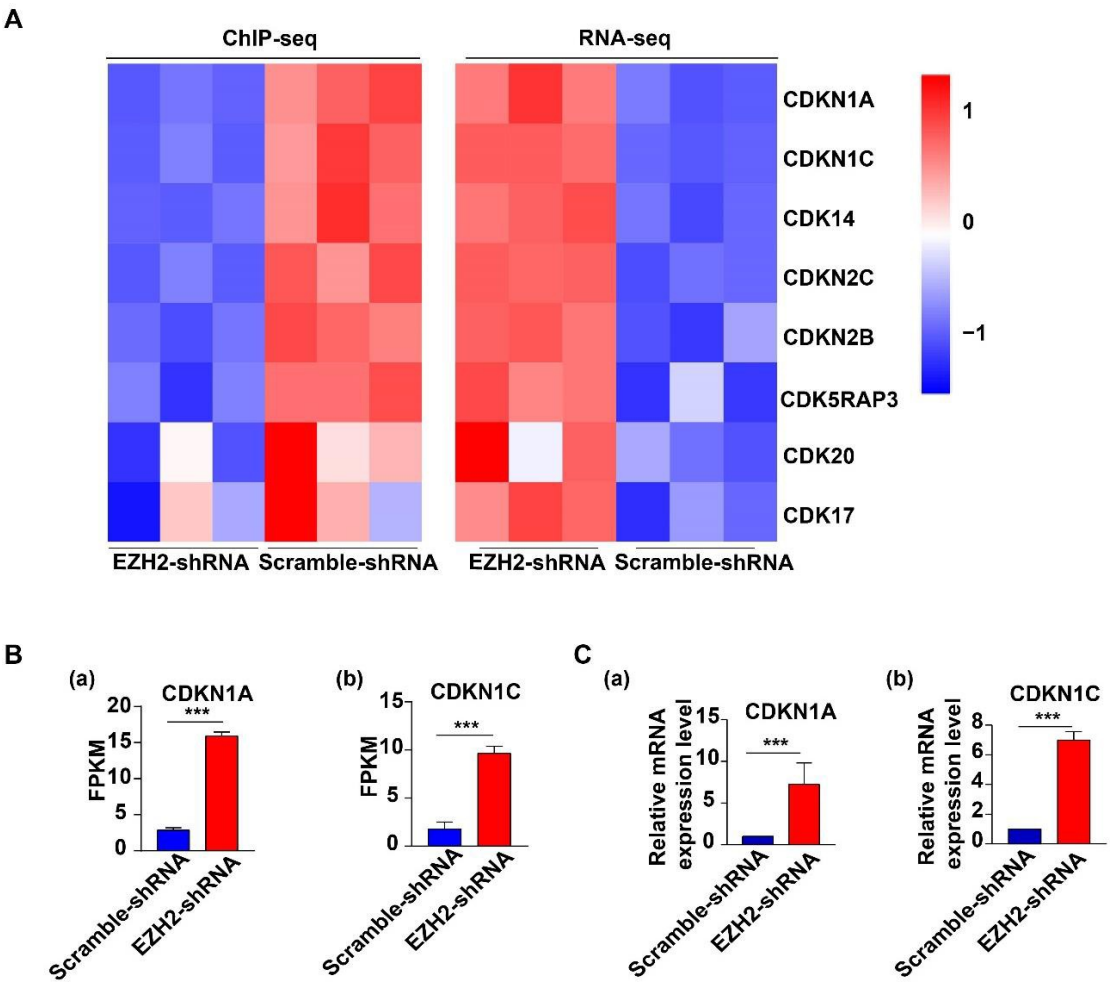

Supplemental Figure 8. Integrated analysis of ChIP-seq and RNA-seq

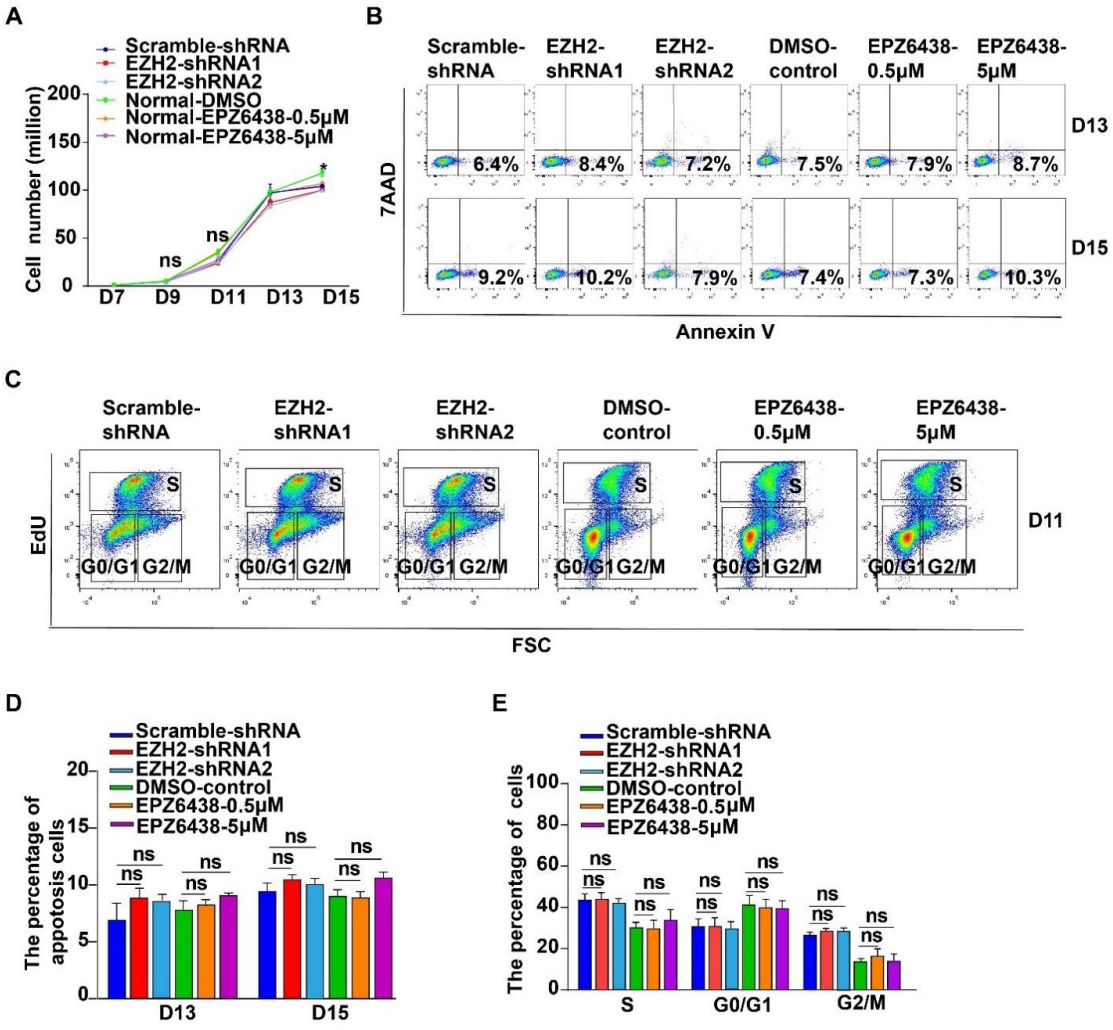

Supplemental Figure 9. EZH2-knockdown did not impair cell growth or apoptosis during terminal erythropoiesis

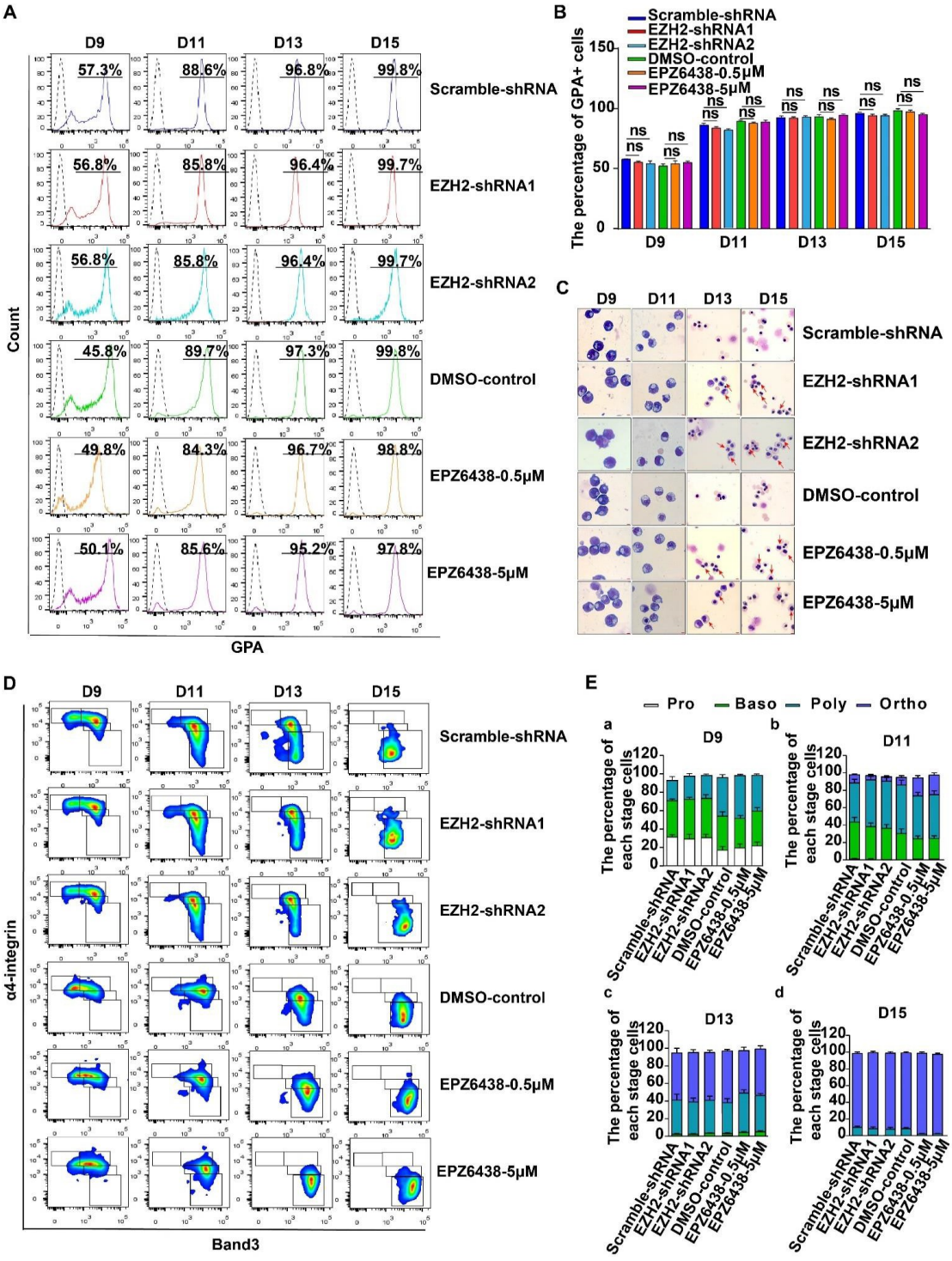

Supplemental Figure 10. EZH2-knockdown has no effect on terminal erythroid differentiation

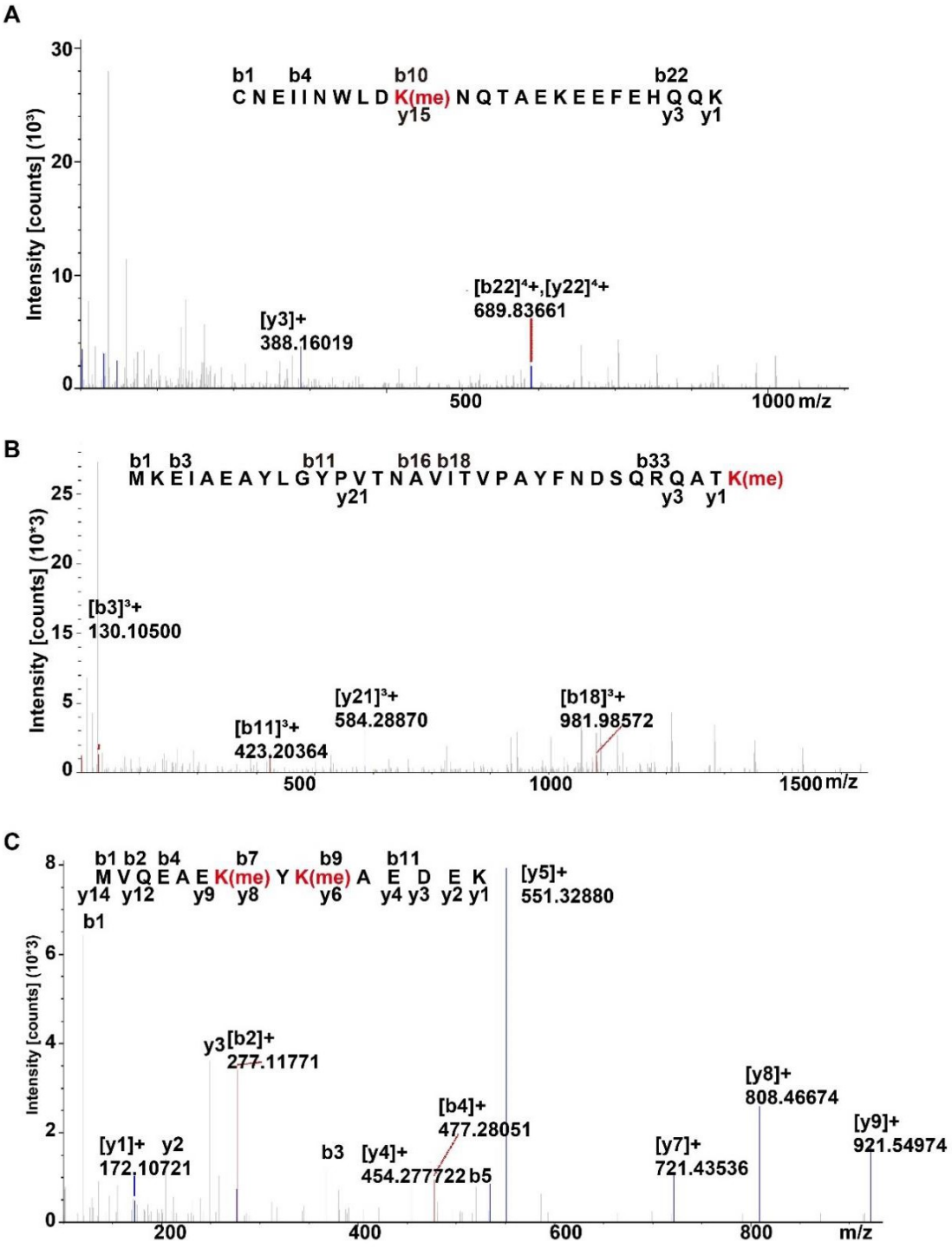

Protein	Sequence	Modifications sites
HSP70	MKEIAEAYLGYPVTNAVITVPAYFNDSQRQATK	K33(Methyl)
	CNEIINWLDKNQTAEKEEFEHQQK	K10(Methyl)
	MVQEAEKYKAEDEK	K7(Methyl); K9(Methyl)

Supplemental Figure 11. Mass spectrometry analysis of HSP70 peptide with HSP70 incubation

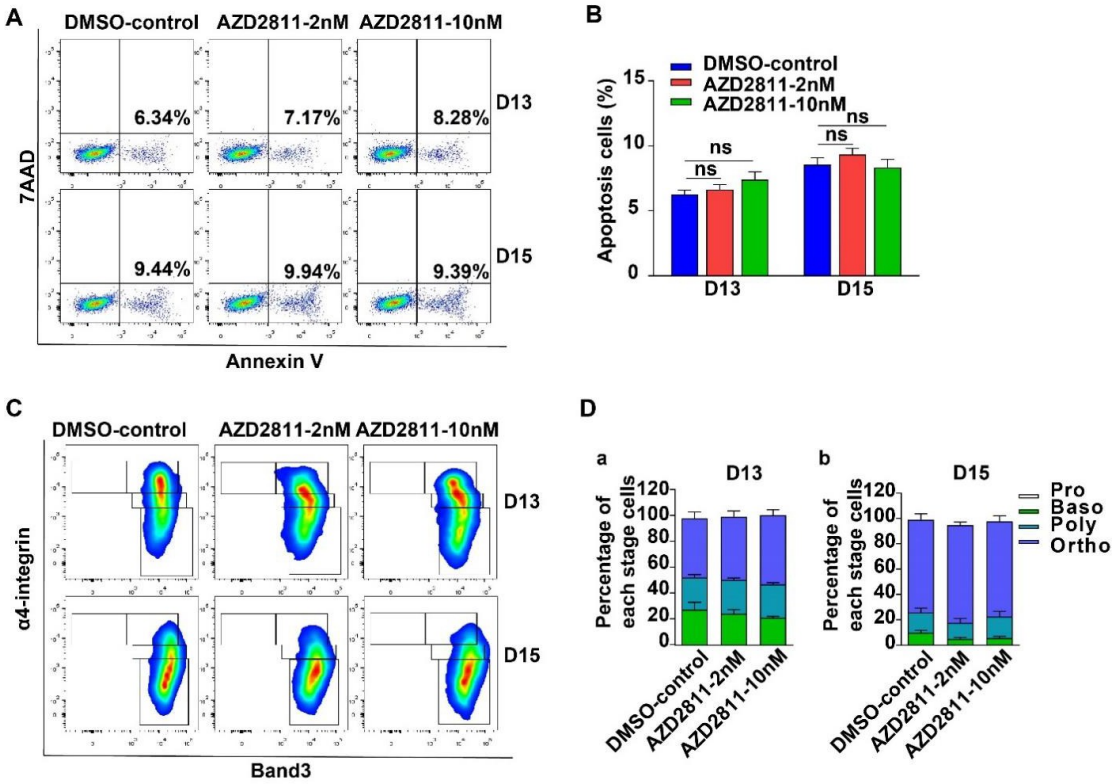

Supplemental Figure 12. AURKB had no effect on cell apoptosis and differentiation during the terminal erythropoiesis.

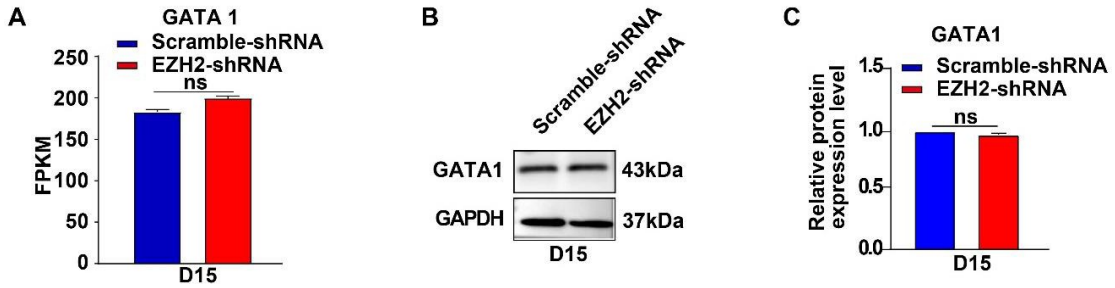

Supplemental Figure 13. Knockdown EZH2 have no effect on the expression of GATA1

Primer		Sequence
EZH2	Forward:	5'AATCAGAGTACATGCGACTGAGA3'
	Reverse:	5'GGAAACAGCGAAGGATACAGC3'
GAPDH	Forward:	5'CATGAGAAGTATGACAACAGCCT3'
	Reverse:	5'AGTCCTTCCACGATACCAAAGT3'
AURKB	Forward:	5'CAGTGGGACACCCGACATC3'
	Reverse:	5'GTACACGTTTCCAAACTTGCC3'

Supplemental table 1. The qRT-PCR primer sequence for EZH2, GAPDH and AURKB